Human Molecular Genetics, 2007, Vol. 16, No. 13 ***1534–1540***
doi:10.1093/hmg/ddm102
Advance Access published on April 27, 2007

In vivo maturation of human frataxin

Ivano Condò[1], Natascia Ventura[1], Florence Malisan[1], Alessandra Rufini[1], Barbara Tomassini[1] and Roberto Testi[1,2,*]

[1]Laboratory of Signal Transduction, Department of Experimental Medicine and Biochemical Sciences, University of Rome 'Tor Vergata', Rome, Italy and [2]Fondazione S. Lucia, Rome, Italy

Received December 21, 2006; Revised March 2, 2007; Accepted April 12, 2007

The defective expression of frataxin causes the hereditary neurodegenerative disorder Friedreich's ataxia (FRDA). Human frataxin is synthesized as a 210 amino acid precursor protein, which needs proteolytic processing into mitochondria to be converted into the functional mature form. *In vitro* processing of human frataxin was previously described to yield a 155 amino acid mature form, corresponding to residues 56–210 (frataxin$^{56-210}$). Here, we studied the maturation of frataxin by *in vivo* overexpression in human cells. Our data show that the main form of mature frataxin is generated by a proteolytic cleavage between Lys80 and Ser81, yielding a 130 amino acid protein (frataxin$^{81-210}$). This maturation product corresponds to the endogenous frataxin detected in human heart, peripheral blood lymphocytes or dermal fibroblasts. Moreover, we demonstrate that frataxin$^{81-210}$ is biologically functional, as it rescues aconitase defects in frataxin-deficient cells derived from FRDA patients. Importantly, our data indicate that frataxin$^{56-210}$ can be produced *in vivo* when the primary 80–81 maturation site is unavailable, suggesting the existence of proteolytic mechanisms that can actively control the size of the mature product, with possible functional implications.

INTRODUCTION

Human frataxin is an ~17 kDa protein, whose deficiency causes Friedreich's ataxia (FRDA), a neurodegenerative disorder characterized by gait and limb ataxia, loss of proprioception, dysarthria, skeletal abnormalities, hypertrophic cardiomyopathy and increased incidence of diabetes (1). In the vast majority of patients (96–98%), the defective expression of frataxin is due to a homozygous GAA triplet repeat expansion within the first intron of the FXN gene, located on chromosome 9q13 (2). The hyperexpansion of GAA repeats determines the formation of a triple helix non-B DNA structure, resulting in an inhibition of frataxin mRNA transcription (3). Moreover, missense mutations are present in FRDA compound heterozygotes, representing 2–4% of patients, which carry an intronic GAA expansions on one FXN allele and a point mutation, mainly located at C-terminal region of frataxin, within exons of the other allele (4).

Frataxin is involved in several aspects of intracellular iron metabolism, such as biogenesis of heme (5) and iron–sulfur clusters (ISCs) (6), iron binding/storage (7) and iron chaperone activity (8). Consequently, frataxin-defective organisms, from unicellular yeast to humans, exhibit a plethora of metabolic disturbances caused by intramitochondrial iron accumulation (9,10), loss of ISC-dependent enzymes (11), reduced oxidative phosphorylation (12) and altered antioxidant defenses (13,14). Moreover, frataxin has a role in controlling cell survival, as underlined by reports documenting that frataxin-deficient cells are more sensitive to oxidative stress (15–17) and that evidence of both apoptotic and autophagic cell death are found in frataxin-deficient animal models (18,19).

The FXN gene encodes for a 210 amino acid protein, representing the precursor form of frataxin (20). The precursor protein contains an N-terminal transit sequence that directs its transport into the mitochondria. Here, a two-step proteolytic processing removes the transit sequence to produce the mature protein. Mitochondrial import and maturation of frataxin is highly conserved during evolution, as documented by several experimental approaches using the yeast, mouse and human frataxin homologs. The first clues on frataxin maturation emerged when physical interaction between mouse frataxin precursor and mouse mitochondrial processing peptidase (MPP) was observed (21). In this report, *in vitro*

*To whom correspondence should be addressed at: Department of Experimental Medicine and Biochemical Sciences, University of Rome 'Tor Vergata', Via Montpellier 1, 00133 Rome, Italy. Tel: +39 0672596503; Fax: +39 0672596505; Email: roberto.testi@uniroma2.it

processing experiments show that recombinant rat MPP cleaves human frataxin to generate an intermediate form lacking the first 40 N-terminal residues. Subsequently, recombinant yeast MPP as well as recombinant rat MPP was shown to operate two sequential cleavages on human frataxin *in vitro* to produce the mature form (22). This two cleavages convert the frataxin precursor first into an ~19 kDa intermediate form and then into an ~17 kDa mature protein. The characterization of such processing products demonstrated that *in vitro* cleavages by MPP occur between Gly41 and Leu42 to yield the intermediate form and between residues Ala55 and Ser56 to generate the mature form of human frataxin (22). However, processing experiments aimed at the identification of the maturation sites in human living cells are still lacking. Here, we analyze the *in vivo* processing of frataxin in human cells. We found that the relevant cleavage responsible for the generation of the major form of mature frataxin *in vivo* occurs between Lys80 and Ser81. The resulting 130 amino acid protein is fully functional, as it can rescue aconitase defects in frataxin-deficient cells. Our data, moreover, indicate that the upstream 55–56 site, previously described *in vitro*, may not be normally used *in vivo*. However, it could be utilized *in vivo* when the primary 80–81 site is unavailable.

RESULTS

Identification of mature frataxin in living cells

In a previous work (17), we generated a frataxin N-terminal deletion mutant lacking the first 55 amino acids (frataxin$^{56-210}$) that remains extramitochondrial when expressed in human cell lines. Although corresponding to the mature frataxin, as defined by *in vitro* processing studies (22), when frataxin$^{56-210}$ is transiently expressed in human cell lines, it migrates slower than the major processing product generated *in vivo* after similar expression of wild-type (WT) frataxin$^{1-210}$. Similarly, when frataxin$^{56-210}$ is stably expressed in frataxin-defective cells derived from FRDA patients, it generates a product that migrates slower than the major form produced *in vivo* after the expression of WT frataxin$^{1-210}$ in the same cells (17). These observations raised the question of whether frataxin$^{56-210}$ truly corresponds to the mature frataxin *in vivo*.

To identify the mature frataxin proteolytically generated in human living cells, SH-SY5Y neuroblastoma cells were transiently transfected with WT frataxin$^{1-210}$ or with frataxin$^{56-210}$ (Fig. 1A). The overexpression of frataxin$^{1-210}$ allows us to detect precursor, intermediate and mature forms. The mature form co-migrates with the endogenous frataxin detectable in untransfected cells. The overexpression of frataxin$^{56-210}$, on the contrary, produces a protein that migrates slower than mature frataxin (Fig. 1A). We also stably expressed WT frataxin$^{1-210}$ or frataxin$^{56-210}$ in HEK-293 cells. Unlike transient expression, which allows us to detect high levels of precursor and intermediate forms, the stable expression of WT frataxin$^{1-210}$ results mainly in the detectable accumulation of the mature product. This clearly co-migrates with the endogenous frataxin detected in human heart, peripheral blood lymphocytes (PBLs) or dermal fibroblasts (Fig. 1B). Here again, the stable expression of frataxin$^{56-210}$ in HEK-293 cells yields a product that migrates slower than the mature form generated from WT frataxin$^{1-210}$. To further analyze this shorter maturation product, mitochondrial and cytosolic fractions were prepared from PBL and from HEK-293 cells stably expressing WT frataxin or frataxin$^{56-210}$. As shown in Figure 1C, the mature frataxin recovered from both mitochondrial and cytosolic fractions of PBL and of HEK-293 cells expressing WT frataxin does not co-migrate with frataxin$^{56-210}$. Together, these results suggest that both mitochondrial and extramitochondrial pools of the human mature frataxin generated *in vivo* are different from that previously identified by *in vitro* processing.

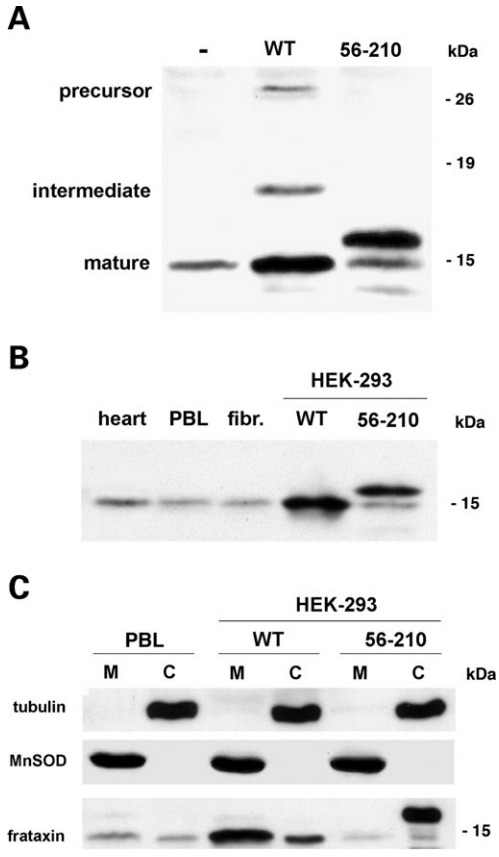

Figure 1. Analysis of the human mature frataxin generated in living cells. Cell extracts were analyzed by 15% SDS–PAGE and immunoblot with anti-frataxin mAb. (**A**) Protein extracts from cultured SH-SY5Y cells (−) and SH-SY5Y cells transiently expressing WT frataxin$^{1-210}$ (WT) or frataxin$^{56-210}$ (56–210). (**B**) Protein extracts from human heart mitochondria (heart), human peripheral lymphocytes (PBL), human skin fibroblasts (fibr.) and HEK-293 cells stably expressing WT frataxin$^{1-210}$ (WT) or frataxin$^{56-210}$ (56–210). (**C**) Mitochondrial (M) and cytosolic (C) fractions from PBL and HEK-293 cells stably expressing WT frataxin$^{1-210}$ (WT) or frataxin$^{56-210}$ (56–210) were analyzed by 15% SDS–PAGE and immunoblot with anti-frataxin mAb.

N-terminal sequencing of the *in vivo* maturation product

HEK-293 cells stably transfected with WT frataxin$^{1-210}$ were used to identify the *in vivo* maturation site of human frataxin. Frataxin was immunopurified from whole-cell extracts,

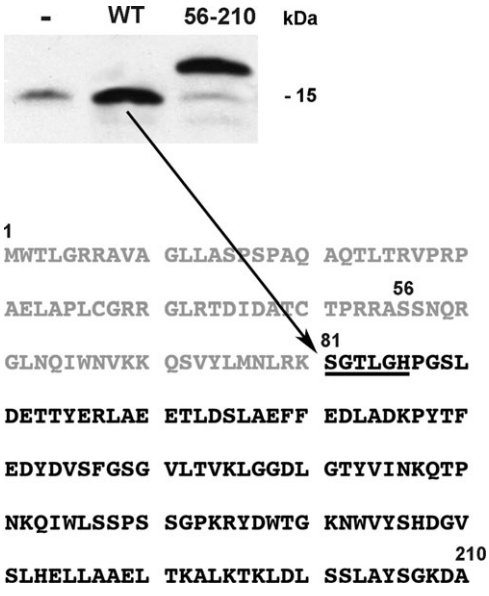

Figure 2. N-terminal sequencing of mature frataxin. Western blot analysis of cell extracts from HEK-293 cells stably transfected with empty vector (−), WT frataxin$^{1-210}$ (WT) or frataxin$^{56-210}$ (56–210). Edman degradation analysis was performed on mature frataxin immunopurified from HEK-293/WT frataxin extracts as described in Materials and Methods. The figure shows the band that was sequenced and the position of the obtained N-terminal residues (underlined) within the frataxin sequence.

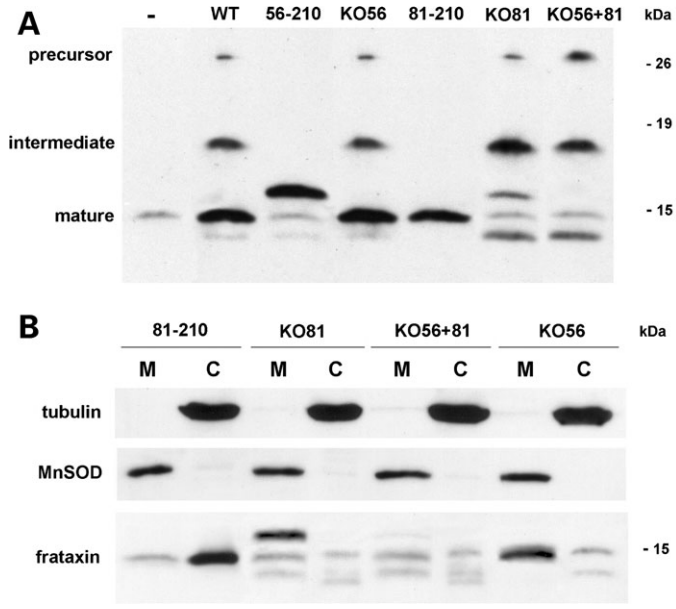

Figure 3. Proteolytic processing of frataxin cleavage mutants. (**A**) SH-SY5Y cells (−) were transiently transfected with WT frataxin$^{1-210}$ (WT), frataxin$^{56-210}$ (56–210), frataxin KO56 mutant (KO56), frataxin$^{81-210}$ (81–210), frataxin KO81 mutant (KO81) or frataxin KO56 + 81 double mutant (KO56 + 81). Cell extracts were analyzed by 15% SDS–PAGE and immunoblot with anti-frataxin mAb. (**B**) Mitochondrial (M) and cytosolic (C) fractions from SH-SY5Y cells transiently transfected with the indicated constructs were analyzed by 15% SDS–PAGE and immunoblot with anti-frataxin mAb.

resolved on SDS–PAGE and subjected to sequential Edman degradation (Fig. 2). N-terminal sequencing yielded the sequence SGTLGH, corresponding to residues 81–86 of human frataxin and indicating that the relevant cleavage occurs between Lys80 and Ser81. Interestingly, the predicted cleavage site matches the R-2 rule used by MPP to recognize most target sequences (23).

Analysis of *in vivo* processing of frataxin cleavage mutants

On the basis of the earlier-mentioned sequencing data, we generated a shorter N-terminal deletion mutant (frataxin$^{81-210}$) and different site-specific mutants of frataxin$^{1-210}$. To abolish the potential cleavage site between residues 80 and 81, a mutant (KO81) was constructed by the substitution of Arg79 and Lys80 with glycine residues. Likewise, to abolish the potential cleavage site Ala55–Ser56, a different mutant (KO56) was obtained by replacing the two arginine residues at positions 53 and 54 with glycines. Finally, an additional mutant (KO56 + 81) combining both mutations was also generated. These mutants were transiently transfected in SH-SY5Y cells, and their *in vivo* maturation was followed. As shown in Figure 3A, the overexpression of the WT frataxin$^{1-210}$ in SH-SY5Y cells results in the accumulation of precursor, intermediate and mature forms, the latter co-migrating with the endogenous frataxin detectable in untransfected cells, whereas the overexpression of frataxin$^{56-210}$ yields a slower migrating product. Importantly, the processing of KO56 mutant is indistinguishable from the processing of WT frataxin$^{1-210}$, suggesting that the 55–56 cleavage site plays a minor role. As predicted, the frataxin$^{81-210}$ deletion mutant gives a product perfectly corresponding to the major maturation product of the WT frataxin$^{1-210}$ and to the endogenous frataxin (Fig. 3A). Accordingly, the KO81 mutant overaccumulates the intermediate form and it is unable to generate mature frataxin, indicating that the 80–81 cleavage site is relevant *in vivo*. Interestingly, the KO81 mutant also allows the accumulation of the 56–210 product, suggesting that the 55–56 site can be functional. Finally, the KO56 + 81 double mutant abrogates both the accumulation of the mature 81–210 product and the alternative 56–210 product and causes overaccumulation of the precursor (Fig. 3A). The severely perturbed maturation of KO81 and KO81 + 56 mutants also results in the appearance of faster migrating products. To address the subcellular distribution of frataxin mutants, mitochondrial and cytosolic fractions were obtained from SH-SY5Y cells transiently transfected as earlier (Fig. 3B). As expected, overexpression of the frataxin$^{81-210}$ construct generates a product that remains extramitochondrial. Importantly, the frataxin$^{56-210}$ product generated from the processing of the overexpressed KO81 mutant mainly resides in the mitochondria (Fig. 3B). This finding suggests that a genuine mitochondrial processing generates the alternative 56–210 product. Together, these data indicate that, in living cells, the primary cleavage site responsible for the generation of mature frataxin occurs between Lys80 and Ser81. However, when the 80–81 site is unavailable, the upstream 55–56 cleavage site can be activated.

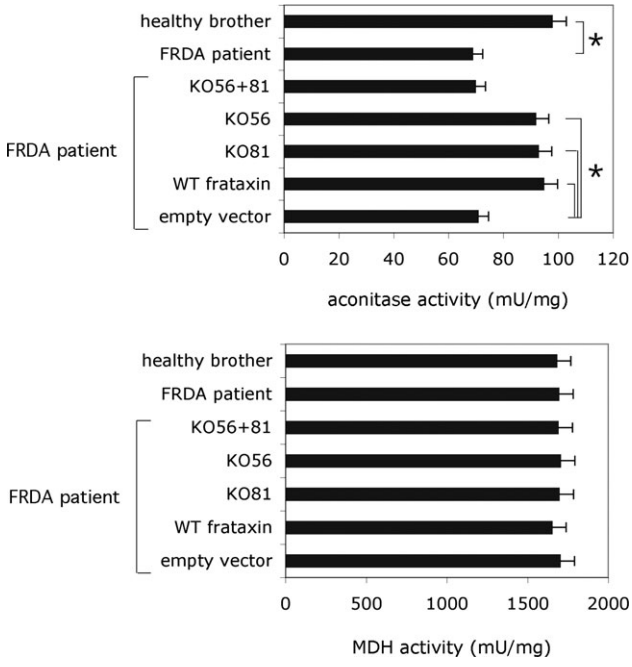

Figure 4. Mature frataxin$^{81-210}$ restores aconitase activity in FRDA cells. Aconitase and malate dehydrogenase assays were performed with cell lysates from lymphoblasts derived from an FRDA patient, from his healthy brother and from the patient lymphoblasts stably reconstituted with empty vector, WT (frataxin$^{1-210}$), frataxin KO56 mutant, frataxin KO81 mutant or frataxin KO56 + 81 double mutant. Means ± 1 SD from three experiments are shown. Asterisk indicates $P < 0.001$.

Frataxin 81–210 rescues aconitase defects in FRDA cells

To further verify that frataxin polypeptide corresponding to residues 81–210 represents an authentic mature protein, we analyzed its functional capability. To this purpose, frataxin-defective lymphoblasts derived from an FRDA patient were stably reconstituted with either the WT frataxin$^{1-210}$ or the processing mutants. Aconitase activity was chosen as a functional readout of frataxin reconstitution, as it has been shown that frataxin-deficient cells have a deficit of numerous ISC-dependent proteins, including aconitase (11,24). Accordingly, cellular extracts from FRDA cells exhibit a significant decrease of aconitase activity with respect to control cells derived from a healthy brother of the patient (Fig. 4). Indeed, aconitase deficit is rescued in FRDA cells reconstituted with WT frataxin$^{1-210}$. Aconitase activity is also restored in FRDA cells reconstituted with the KO56 mutant, which is capable of generating the 81–210 frataxin product, as well as in cells expressing the KO81 mutant, which generates the 56–210 product (Fig. 4). On the other hand, aconitase activity could not be restored in FRDA cells reconstituted with the KO56 + 81 mutant, unable to generate both maturation products. Measured as a control, the activity of malate dehydrogenase, another enzyme involved in the tricarboxylic acid cycle, but lacking ISC, did not change with the expression levels of mature frataxin (Fig. 4).

Thus, our data strongly indicate that the 130 residue-long frataxin$^{81-210}$ is biologically functional and it represents a genuine mature product in human cells.

DISCUSSION

Human frataxin is a highly conserved, nuclear-encoded protein, which needs proteolytic processing to be converted into the functional mature form. Indeed, in eukaryotes, frataxin is synthesized as a pre-protein containing an N-terminal signal peptide for its transport to the mitochondria. The yeast frataxin precursor Yfh1p is proteolytically maturated with two sequential cleavages by MPP (25). The first cleavage removes 20 N-terminal residues, containing the mitochondrial signal peptide, to generate an intermediate form. This product is then subjected to a second step that cleaves off a spacer sequence constituted by residues 21–51, yielding the 123 amino acid mature Yfh1p (25). The maturation of human frataxin precursor was described to occur through either a one- or a two-step reaction catalyzed by MPP. The one-step model was proposed on the basis of import and maturation of *in vitro*-translated precursor into purified yeast or rat mitochondria. These data, as also supported by *in vitro*-processing reactions with recombinant yeast or rat MPP, report a single cleavage product (26). The opposite two-step model derives from the analysis of frataxin cleavage by recombinant yeast or rat MPP and within isolated rat mitochondria (22). This latter study characterizes two MPP cleavage sites by N-terminal radiosequencing of the products of the *in vitro*-translated precursor processed by recombinant yeast enzyme. The first cleavage removes 41 N-terminal residues to generate the intermediate frataxin, whereas the second step removes a 14-residue linker peptide, yielding the 155 amino acid mature frataxin (frataxin$^{56-210}$). However, both approaches make use of *in vitro* heterologous systems. Given the lack of information in living cells, we studied the maturation of human frataxin by *in vivo* overexpression in human cells. Although our data agree with the two-step processing model, they suggest a different identity for the human mature frataxin. We generated HEK-293 cells stably expressing WT frataxin$^{1-210}$ or a truncated form corresponding to the previously described mature protein (frataxin$^{56-210}$). Notably, the frataxin$^{56-210}$ polypeptide does not co-migrate either with the mature form generated by frataxin$^{1-210}$ expressing cells or with the endogenous frataxin detected in human primary cells or human tissues. Accordingly, Edman degradation analysis of immunopurified mature frataxin from HEK-293 cells demonstrates that the N-terminal sequence matches residues starting from Ser81 instead of Ser56. Interestingly, although not directly addressed in this work, the cleavage between Lys80 and Ser81 is a potential MPP target (27). In fact, the upstream sequence contains a proximal basic arginine at the P2 position (Arg79) and distal N-terminal basic residues, generally between 3 and 10 amino acids (Lys69 and Lys70) from the proximal Arg79. Moreover, this sequence shows a polar residue at position P3′ (Thr83), but lacks a hydrophobic residue at position P1′. Accordingly, the glycine substitution of Arg79 and Lys80 completely blocks the last maturation step of the KO81 mutant. It is worthwhile mentioning that inhibition of processing at Ser81 site allows the accumulation of a novel cleavage product that co-migrates with the polypeptide 56–210. In fact, this form is absent in the processing of the KO56 + 81 mutant. It is therefore possible that the cryptic 55–56 site is used when the primary 80–81

site is somehow unavailable. This anyhow results in the generation of a functional frataxin, as frataxin$^{56-210}$ from KO81 mutant can functionally reconstitute aconitase activity (Fig. 4) and resistance to oxidative stress in frataxin-defective cells derived from FRDA patients (17). The activation of a cryptic cleavage site, when the canonical site is abolished, has been described for the MPP-mediated maturation of ornithine transcarbamylase (28).

Our results show a clear discrepancy between *in vivo* and *in vitro* processing of human frataxin. A possible explanation could be represented by the preferential choice of a different processing site in heterologous systems. Rat and human MPPs show a high degree of sequence homology (23); nevertheless, a species-specific substrate recognition by this peptidase cannot be excluded. Moreover, the previously reported N-terminal sequencing of the human mature frataxin was performed on the product processed *in vitro* by yeast MPP (22).

A key information from our results is the ability of mature frataxin$^{81-210}$ to rescue metabolic defects in frataxin-deficient cells. In fact, reconstitution of frataxin-defective cells derived from FRDA patients with the KO56 mutant, unable to produce frataxin$^{56-210}$, but still competent to generate frataxin$^{81-210}$, clearly restores the aconitase deficit. The defective activity of ISC-dependent proteins such as mitochondrial and cytosolic aconitase, as well as of the subunits of respiratory complexes, is clearly associated with frataxin deficiency in several model organisms and in FRDA patients (11,24,29,30). Moreover, many evidence support the direct function of frataxin in controlling aconitase activity by iron delivery and reactivation of its damaged ISC (8,31,32). Thus, frataxin$^{81-210}$ is a functional processing product that is not generated from the degradation of frataxin$^{56-210}$ *in vivo*, since no frataxin$^{56-210}$ is made during the processing of the KO56 mutant. Accordingly, the transient or stable overexpression of frataxin$^{56-210}$ in several cell types never resulted in the appearance of the 81–210 product (17 and this study).

It has been reported that recombinant human frataxin purified from *Escherichia coli* undergoes 'spontaneous' proteolysis yielding shorter forms devoid of the non-conserved N-terminal region (31,33–35). These more stable products have been used to define the structure of frataxin by NMR (33) and X-ray crystallography (34). It is important to note that an autoproteolytic form of frataxin was found to extend from residues 78 to 210 (7,35), intriguingly similar to the mature product identified *in vivo* by our study. This 78–210 form was shown to be fully functional as demonstrated by its ability to bind and to deliver ferrous iron for ISC (31) and heme biosynthesis (5). However, *in vitro* self-assembly experiments suggest a critical role played by residues spanning from 56 to 78 in frataxin polymers formation (36). The *in vivo* relevance of frataxin homopolymerization was recently analyzed in the yeast knockout model Δ*yfh1* (37,38). Oligomerization-deficient Yfh1p mutants were shown to rescue the growth defect of Δ*yfh1* cells, similar to the WT protein, and to interact with the Fe/S scaffold Isu (37), thus indicating that frataxin homopolymerization is dispensable in living yeast. However, in Yfh1p mutants lacking ferroxidase or mineralization activity, which are distinctive of the frataxin polymers, iron-induced oxidative stress is increased and life span is reduced, independently of the iron chaperone capability (38).

In humans, the *in vivo* role of frataxin polymers in iron storage and detoxification has not been clarified. Our data support the view that frataxin$^{81-210}$ is the primary mature form generated *in vivo*, probably designed to act as a monomeric iron chaperone. However, we show that frataxin$^{56-210}$ can be proteolytically produced from the precursor *in vivo* when the primary 80–81 site is blocked. This finding opens the possibility that, under conditions that would require enhanced frataxin-mediated iron storage or iron detoxification, the alternative 55–56 site could be activated to allow the production of a frataxin with oligomerization capability. Further analysis will be eventually required to elucidate the mechanisms that might control the molecular shift between the monomeric iron chaperone and the polymeric iron storage status of human frataxin.

MATERIALS AND METHODS

Frataxin expression constructs

The pIRES2/FXN$^{1-210}$ and pIRES2/FXN$^{56-210}$ constructs were previously described (17). The pIRES2/FXN$^{81-210}$ construct was synthesized by PCR using the primers 5′-CTAGGAATTCATGTCTGGAACTTTGGGCCACCC-3′ (*Eco*RI) and 5′-AGTTGGATCCGCATCAAGCATCTTTTC CGG-3′ (*Bam*HI), in order to remove the first 80 amino acid from frataxin precursor, and inserted in pIRES2-EGFP vector (BD Clontech). The FXN$^{1-210}$ and FXN$^{56-210}$ cDNAs were cloned into *Hin*dIII and *Bam*HI sites of the vector pcDNA5/FRT (Invitrogen) to obtain the stable expression in Flp-In-293 cells (Invitrogen). The mutant constructs pIRES2/FXN_KO56, pIRES2/FXN_KO81 and pIRES2/FXN_KO56 + 81 were generated using the QuickChange site-directed mutagenesis kit (Stratagene) using pIRES2/FXN$^{1-210}$ as template. All final constructs were verified by DNA sequencing.

Cell cultures and transfections

GM15850B lymphoblasts, from a clinically affected FRDA patient, homozygous for the GAA expansion in the FXN gene with alleles containing ~700 and 1050 repeats, and GM15851B lymphoblasts from a clinically unaffected brother of GM15850, with two FXN alleles in the normal range of GAA trinucleotide repeats, were obtained from NIGMS Human Genetic Cell Repository, Coriell Institute for Medical Research. Cells were maintained in RPMI 1640 medium supplemented with 15% FBS and transfected by electroporation. Briefly, 10^7 cells were incubated in 0.4 ml of RPMI 1640 for 10 min on ice with 30 μg of pIRES2/FNX mutant constructs. After electroporation at 260 V/950 μF, cells were left 30 min on ice and resuspended in 5 ml of RPMI 1640, 15% FBS. After 4 h, live cells were recovered by Lympholyte-H (Cedarlane Laboratories) density gradient centrifugation and replated. Stable transfectants were obtained from cultures in selection medium containing 500 μg/ml G418 (Invitrogen) for 15–20 days. Flp-In-293 cells (Invitrogen) are human embryonic kidney HEK-293 variants allowing the stable integration and expression of a transfected gene. Flp-In-293 cells were maintained in DMEM medium

supplemented with 10% FBS and transfected with the calcium phosphate precipitation method. Briefly, cells were plated on 10 cm dishes and co-transfected with 10 μg total DNA. After 16 h, the medium was replaced with a fresh one. The 293 clones stably expressing FXN^{1-210} or FXN^{56-210} were obtained from cultures in selection medium containing 100 μg/ml hygromycin B (Invitrogen). Bone marrow neuroblastoma SH-SY5Y cells were maintained in RPMI 1640 medium containing 10% FBS and transiently transfected using Lipofectamine 2000 (Invitrogen), following the manufacturer's instructions. Human PBLs from different healthy donors were isolated by lymphoprep density gradient centrifugation at 800*g*. Cultured skin fibroblasts from healthy donors were provided by Dr G. Novelli (University of Rome 'Tor Vergata', Italy).

Purification and N-terminal sequencing of mature frataxin

Total cell lysates from Flp-In-293 cells stably expressing FXN WT were prepared in RIPA buffer (50 mM Tris–HCl pH 7.5, 150 mM NaCl, 1% NP-40, 1% sodium deoxycholate, 0.1% SDS, 5 mM EDTA) containing Complete protease inhibitor cocktail (Roche Diagnostics). Frataxin was immunoprecipitated from ~60 mg of the whole extract with mAb anti-frataxin 1G2 (Immunological Sciences) and protein G-sepharose beads (GE Healthcare Life Sciences). Immunocomplexes were then resolved by 15% SDS–PAGE, and coomassie-stained bands were excised from the gel. N-terminal amino acid sequence was determined by automated Edman degradation performed by Alta Bioscience (University of Birmingham, UK).

Western blotting

To prepare total protein lysates, cells were washed twice with ice-cold PBS and lysed in ice-cold RIPA buffer supplemented with Complete protease inhibitor cocktail. Mitochondrial and cytosolic extracts were prepared as described (17). The human heart mitochondrial sample was prepared post-mortem from a donor (Immunological Sciences). Cell extracts were separated by 15% SDS–PAGE and analyzed by immunoblotting with mAb anti-frataxin (Immunological Sciences), mAb anti-α-Tubulin (Sigma) and anti-Mn SOD (StressGen) using ECL system detection (GE Healthcare Life Sciences).

Enzyme assays

Aconitase activity was measured spectrophotometrically at 340 nm by a coupled reaction of aconitase and isocitrate dehydrogenase. Total cell extracts were obtained by lysis in HDGC buffer (20 mM Hepes, pH 7.4, 1 mM DTT, 10% glycerol, 2 mM sodium citrate, 1% triton X-100) supplemented with Complete protease inhibitor cocktail. The assay reactions contained 100 μg of cell lysate in 50 mM Hepes, pH 7.4, 1 mM sodium citrate, 0.6 mM $MnCl_2$, 0.2 mM $NADP^+$ and 2 U/ml isocitrate dehydrogenase from porcine heart (Sigma-Aldrich). Malate dehydrogenase activity was assessed by following the oxidation of NADH at 340 nm. The reaction mixtures contained 50 μg of cell lysate in 50 mM Tris–HCl, pH 7.5, 0.1 mM NADH and 0.4 mM oxaloacetic acid.

For the calculation of the activities, 1 mU of enzyme was defined as the amount of protein that converted 1 nmol of $NADP^+$ (aconitase) or NADH (malate dehydrogenase) in 1 min. Statistical analysis was performed using Student's *t*-test; all values are expressed as means ± SD.

ACKNOWLEDGEMENTS

Thanks are due to Dario Serio for his technical assistance. This work has been supported by the Associazione Italiana Ricerca sul Cancro, the European Commission (Project TRANSDEATH), National Ataxia Foundation, Ataxia UK and Friedreich's Ataxia Research Alliance. The financial support of Telethon-Italy (Grant GGP06059) is gratefully acknowledged.

Conflict of Interest statement. None declared.

REFERENCES

1. Pandolfo, M. (2003) Friedreich ataxia. *Semin. Pediatr. Neurol.*, **10**, 163–172.
2. Campuzano, V., Montermini, L., Molto, M.D., Pianese, L., Cossee, M., Cavalcanti, F., Monros, E., Rodius, F., Duclos, F., Monticelli, A. *et al.* (1996) Friedreich's ataxia: autosomal recessive disease caused by an intronic GAA triplet repeat expansion. *Science*, **271**, 1423–1427.
3. Sakamoto, N., Ohshima, K., Montermini, L., Pandolfo, M. and Wells, R.D. (2001) Sticky DNA, a self-associated complex formed at long GAA*TTC repeats in intron 1 of the frataxin gene, inhibits transcription. *J. Biol. Chem.*, **276**, 27171–27177.
4. Cossée, M., Durr, A., Schmitt, M., Dahl, N., Trouillas, P., Allinson, P., Kostrzewa, M., Nivelon-Chevallier, A., Gustavson, K.H., Kohlschutter, A. *et al.* (1999) Friedreich's ataxia: point mutations and clinical presentation of compound heterozygotes. *Ann. Neurol.*, **45**, 200–206.
5. Yoon, T. and Cowan, J.A. (2004) Frataxin-mediated iron delivery to ferrochelatase in the final step of heme biosynthesis. *J. Biol. Chem.*, **279**, 25943–25946.
6. Stehling, O., Elsasser, H.P., Bruckel, B., Muhlenhoff, U. and Lill, R. (2004) Iron–sulfur protein maturation in human cells: evidence for a function of frataxin. *Hum. Mol. Genet.*, **13**, 3007–3015.
7. Cavadini, P., O'Neill, H.A., Benada, O. and Isaya, G. (2002) Assembly and iron-binding properties of human frataxin, the protein deficient in Friedreich ataxia. *Hum. Mol. Genet.*, **11**, 217–227.
8. Bulteau, A.L., O'Neill, H.A., Kennedy, M.C., Ikeda-Saito, M., Isaya, G. and Szweda, L.I. (2004) Frataxin acts as an iron chaperone protein to modulate mitochondrial aconitase activity. *Science*, **305**, 242–245.
9. Babcock, M., de Silva, D., Oaks, R., Davis-Kaplan, S., Jiralerspong, S., Montermini, L., Pandolfo, M. and Kaplan, J. (1997) Regulation of mitochondrial iron accumulation by Yfh1p, a putative homolog of frataxin. *Science*, **276**, 1709–1712.
10. Bradley, J.L., Blake, J.C., Chamberlain, S., Thomas, P.K., Cooper, J.M. and Schapira, A.H. (2000) Clinical, biochemical and molecular genetic correlations in Friedreich's ataxia. *Hum. Mol. Genet.*, **9**, 275–282.
11. Rotig, A., de Lonlay, P., Chretien, D., Foury, F., Koenig, M., Sidi, D., Munnich, A. and Rustin, P. (1997) Aconitase and mitochondrial iron–sulphur protein deficiency in Friedreich ataxia. *Nat. Genet.*, **17**, 215–217.
12. Ristow, M., Pfister, M.F., Yee, A.J., Schubert, M., Michael, L., Zhang, C.Y., Ueki, K., Michael, M.D., II., Lowell, B.B. and Kahn, C.R. (2000) Frataxin activates mitochondrial energy conversion and oxidative phosphorylation. *Proc. Natl Acad. Sci. USA*, **97**, 12239–12243.
13. Chantrel-Groussard, K., Geromel, V., Puccio, H., Koenig, M., Munnich, A., Rotig, A. and Rustin, P. (2001) Disabled early recruitment of antioxidant defenses in Friedreich's ataxia. *Hum. Mol. Genet.*, **10**, 2061–2067.
14. Jiralerspong, S., Ge, B., Hudson, T.J. and Pandolfo, M. (2001) Manganese superoxide dismutase induction by iron is impaired in Friedreich ataxia cells. *FEBS Lett.*, **509**, 101–105.

15. Wong, A., Yang, J., Cavadini, P., Gellera, C., Lonnerdal, B., Taroni, F. and Cortopassi, G. (1999) The Friedreich's ataxia mutation confers cellular sensitivity to oxidant stress which is rescued by chelators of iron and calcium and inhibitors of apoptosis. *Hum. Mol. Genet.*, **8**, 425–430.
16. Tan, G., Chen, L.S., Lonnerdal, B., Gellera, C., Taroni, F.A. and Cortopassi, G.A. (2001) Frataxin expression rescues mitochondrial dysfunctions in FRDA cells. *Hum. Mol. Genet.*, **10**, 2099–2107.
17. Condò, I., Ventura, N., Malisan, F., Tomassini, B. and Testi, R. (2006) A pool of extramitochondrial frataxin that promotes cell survival. *J. Biol. Chem.*, **281**, 16750–16756.
18. Cossée, M., Puccio, H., Gansmuller, A., Koutnikova, H., Dierich, A., LeMeur, M., Fischbeck, K., Dolle, P. and Koenig, M. (2000) Inactivation of the Friedreich ataxia mouse gene leads to early embryonic lethality without iron accumulation. *Hum. Mol. Genet.*, **9**, 1219–1226.
19. Simon, D., Seznec, H., Gansmuller, A., Carelle, N., Weber, P., Metzger, D., Rustin, P., Koenig, M. and Puccio, H. (2004) Friedreich ataxia mouse models with progressive cerebellar and sensory ataxia reveal autophagic neurodegeneration in dorsal root ganglia. *J. Neurosci.*, **24**, 1987–1995.
20. Bencze, K.Z., Kondapalli, K.C., Cook, J.D., McMahon, S., Millan-Pacheco, C., Pastor, N. and Stemmler, T.L. (2006) The structure and function of frataxin. *Crit. Rev. Biochem. Mol. Biol.*, **41**, 269–291.
21. Koutnikova, H., Campuzano, V. and Koenig, M. (1998) Maturation of wild-type and mutated frataxin by the mitochondrial processing peptidase. *Hum. Mol. Genet.*, **7**, 1485–1489.
22. Cavadini, P., Adamec, J., Taroni, F., Gakh, O. and Isaya, G. (2000) Two-step processing of human frataxin by mitochondrial processing peptidase. Precursor and intermediate forms are cleaved at different rates. *J. Biol. Chem.*, **275**, 41469–41475.
23. Gakh, O., Cavadini, P. and Isaya, G. (2002) Mitochondrial processing peptidases. *Biochim. Biophys. Acta.*, **1592**, 63–77.
24. Rouault, T.A. and Tong, W.H. (2005) Iron–sulphur cluster biogenesis and mitochondrial iron homeostasis. *Nat. Rev. Mol. Cell. Biol.*, **6**, 345–351.
25. Branda, S.S., Cavadini, P., Adamec, J., Kalousek, F., Taroni, F. and Isaya, G. (1999) Yeast and human frataxin are processed to mature form in two sequential steps by the mitochondrial processing peptidase. *J. Biol. Chem.*, **274**, 22763–22769.
26. Gordon, D.M., Shi, Q., Dancis, A. and Pain, D. (1999) Maturation of frataxin within mammalian and yeast mitochondria: one-step processing by matrix processing peptidase. *Hum. Mol. Genet.*, **8**, 2255–2262.
27. Taylor, A.B., Smith, B.S., Kitada, S., Kojima, K., Miyaura, H., Otwinowski, Z., Ito, A. and Deisenhofer, J. (2001) Crystal structures of mitochondrial processing peptidase reveal the mode for specific cleavage of import signal sequences. *Structure*, **9**, 615–625.
28. Sztul, E.S., Hendrick, J.P., Kraus, J.P., Wall, D., Kalousek, F. and Rosenberg, L.E. (1987) Import of rat ornithine transcarbamylase precursor into mitochondria: two-step processing of the leader peptide. *J. Cell. Biol.*, **105**, 2631–2639.
29. Puccio, H., Simon, D., Cossée, M., Criqui-Filipe, P., Tiziano, F., Melki, J., Hindelang, C., Matyas, R., Rustin, P. and Koenig, M. (2001) Mouse models for Friedreich ataxia exhibit cardiomyopathy, sensory nerve defect and Fe–S enzyme deficiency followed by intramitochondrial iron deposits. *Nat. Genet.*, **27**, 181–186.
30. Chen, O.S., Hemenway, S. and Kaplan, J. (2002) Inhibition of Fe–S cluster biosynthesis decreases mitochondrial iron export: evidence that Yfh1p affects Fe–S cluster synthesis. *Proc. Natl Acad. Sci. USA*, **99**, 12321–12326.
31. Yoon, T. and Cowan, J.A. (2003) Iron–sulfur cluster biosynthesis. Characterization of frataxin as an iron donor for assembly of [2Fe–2S] clusters in ISU-type proteins. *J. Am. Chem. Soc.*, **125**, 6078–6084.
32. Bulteau, A.L., Lundberg, K.C., Ikeda-Saito, M., Isaya, G. and Szweda, L.I. (2005) Reversible redox-dependent modulation of mitochondrial aconitase and proteolytic activity during *in vivo* cardiac ischemia/reperfusion. *Proc. Natl Acad. Sci. USA*, **102**, 5987–5991.
33. Musco, G., Stier, G., Kolmerer, B., Adinolfi, S., Martin, S., Frenkiel, T., Gibson, T. and Pastore, A. (2000) Towards a structural understanding of Friedreich's ataxia: the solution structure of frataxin. *Struct. Fold. Des.*, **8**, 695–707.
34. Dhe-Paganon, S., Shigeta, R., Chi, Y.I., Ristow, M. and Shoelson, S.E. (2000) Crystal structure of human frataxin. *J. Biol. Chem.*, **275**, 30753–30756.
35. Yoon, T., Dizin, E. and Cowan, J.A. (2007) N-terminal iron-mediated self-cleavage of human frataxin: regulation of iron binding and complex formation with target proteins. *J. Biol. Inorg. Chem.*, **12**, 535–542.
36. O'Neill, H.A., Gakh, O. and Isaya, G. (2005) Supramolecular assemblies of human frataxin are formed via subunit–subunit interactions mediated by a non-conserved amino-terminal region. *J. Mol. Biol.*, **345**, 433–439.
37. Aloria, K., Schilke, B., Andrew, A. and Craig, E.A. (2004) Iron-induced oligomerization of yeast frataxin homologue Yfh1 is dispensable *in vivo*. *EMBO Rep.*, **5**, 1096–1101.
38. Gakh, O., Park, S., Liu, G., Macomber, L., Imlay, J.A., Ferreira, G.C. and Isaya, G. (2006) Mitochondrial iron detoxification is a primary function of frataxin that limits oxidative damage and preserves cell longevity. *Hum. Mol. Genet.*, **15**, 467–479.